บรรณานุกรม

Batiste, S. N., Alshibli, K. A., Stureb S. and Lankton, M. (2004) Shear band characterization of triaxial sand specimens using computed tomography. Geotechnical testing Journal, 27(6), 568 – 579.

Blewett, J., Blewett, I. J., and Woodward, P. K. (1999) Measurement of shear-wave velocity using phase-sensitive detection techniques. Canadian Geotechnical Journal. 36(5): 934-939.

Desrues, J. Chambon, M., Mokni, M. and Mazerolle, F. (1996):"Void ratio evolution inside shear bands in triaxial sand specimens studied by computed tomography," Geotechnique 46(3), 529 – 546.

Desrues, J. 2004. Tracking strain localization in geomaterials using computerized tomography. in Omani, J. and Obara, Y. (Eds). Proceedings of the International Workshop on X-ray CT for Geomaterials, 15-41. International Workshop on X-ray CT for Geomaterials, November 6-7, 2003. Kumamoto, Japan. Balkema.

Finno, R., Harris, W., Mooney, M., and Vagina G. 1997. Shear bands in plane strain compression of loose sand. Géotechnique 47(1): 149-165.

Gudehus, G. and Nubel, K. (2004). Evolution of shear bands in sand. Geotechnique 54 No. 3, 187 – 201.

Hardin, B.O. and Richart, F.E. 1963. Elastic Wave Velocities in Granular Soils. Journal of Soil Mechanics and Foundations Division. (89)SM1: 33-65. ASCE.

Jovicic, V., Coop, M.R., and Simic, M. 1996. Objective criteria for determining G_{max} from bender element tests. Geotechnique. 46(2): 357-362.

Kodaka, T., Higo, Y., Kimoto, S. and Oka, F. (2007): Effects of sample shape on the strain localization of water-saturated clay, International Journal for Numerical and Analytical Methods in Geomechanics, 31(3), 483 – 521.

Kumar, J., and Madhusudhan, B. N. (2010) A note on the measurement of travel times using bender and extender elements. Soil Dynamics and Earthquake Engineering. 30(2010): 630–634.

Lesniewska, D. and Mroz, Z. (2000): Limit equilibrium approach to study the evolution of shear band systems in soils. Geotechnique, 50(5), 521 – 536.

Sachan, A. and Penumadu, D. 2007. Strain localization in solid cylindrical clay specimens using Digital Image Analysis (DIA) technique. Soils and Foundations. 47(1): 67-78.

Santamarina, J.C. and Cascante, G. 1996. Stress anisotropy and wave propagation - A micromechanical view. Canadian Geotechnical Journal. 33(5): 770-782.

Santamarina J.C., Klein K.A., and Fam, M.A. 2001. Soils and Waves: Particulate Materials Behaviour, Characterisation and Process Monitoring. J. Wiley & Sons, 508 pages.

Lee J.S. and Santamarina J.C. 2005. Bender Elements: Performance and Signal Interpretation. Journal of Geotechnical and Geoenvironmental Engineering. 131(9): 1063-1070.

Leong, E.C., Yeo, S.H., Rahardjo, H. (2005): Measuring Shear Wave Velocity Using Bender Elements. Geotechnical Testing Journal, 28, 5: 488-498.

Minsu, C., and Gye-Chun, C. (2007): Shear Strength Estimation of Sandy Soils Using Shear Wave Velocity. Geotechnical Testing Journal (GTJ), 30(6) 484-495.

Mostafa A. Ismail, Shambhu S. Sharma and Martin Fahey. (2005). A Small True Triaxial Apparatus with Wave Velocity Measurement. Geotechnical Testing Journal, Vol.28, No.2. ASTM International.

Roscoe, K. H. (1970). The influence of strains in soil mechanics. Geotechnique 20, 129 – 170.

Sachan, A. and Penumadu, D. (2007): Strain localization in solid cylindrical clay specimens using Digital Image Analysis (DIA) technique. Soils and Foundations, 47(1), 67 – 78.

Sanchez-Salinero, I., Roesset, J.M., and Stokoe, K.H. 1986. Analytical studies of body wave propagation and attenuation. Report GR 86-15. Civil Engineering Department, University of Texas at Austin, TX.

Shirley, D.J., and Hampton, L.D. (1977): Shear wave measurements in laboratory sediments. Journal of the Acoustic Society of American, 63(5), 607-613.

Teachavorasinskun, S. and Akkarakun, T. (2004): "Paths of elastic shear modulus of clays," Geotechnique 54, No.5, 331-333.

Teachavorasinskun, S. and Amornwithayalax, T. (2002): "Elastic shear modulus of Bangkok clay during undrained triaxial compression," Geotechnique 52, No. 7, 537-540.

Wanatowski, D. and Chu, J. (2006): Stress-strain behavior of a granular fill measured by a new plane-strain apparatus. Geotechnical Testing Journal, 29(2), 149 – 157.

Editorial Manager(tm) for Geotechnique
Manuscript Draft

Manuscript Number: 11-T-002

Title: Identification of localization in sandy soils using shear wave logging

Article Type: Technical Note

Corresponding Author: Supot Teachavorasinskun, Ph.D.

Corresponding Author's Institution: Chulalongkorn University

First Author: Supot Teachavorasinskun, Ph.D.

Order of Authors: Supot Teachavorasinskun, Ph.D.;Pulpong Pongvithayapanu, Ph. D

Abstract: Since shear wave velocity and strain localization are influenced by some common factors, it is very likely that these two phenomena can be correlated. In the present study, strain localization of sandy soils was indirectly explored using the shear wave propagation characteristics and simple digital image analysis in drained traxial compression. It was found that shear wave velocity of the tested sample undergone high stress ratio exhibited a linear reduction against axial strain. The global strains levels at which shear wave started to travel at a decreasing velocity were ranged between 2 - 5%. These were smaller than that required for sample to attain the peak stress ratio. It implied that localization was induced before sample reaching its peak stress ratio. The characteristics of shear wave velocity can fairly well detect the initialization of shear band.

Number of words = 2,700
Number of figure = 10
Number of Table = 2

Suggested Reviewers:

Opposed Reviewers:

January 7, 2011

Manuscript submitted for possible publication as a ***Technical Note*** in *Geotechnique*

Identification of localization in sandy soils using shear wave logging

By

Supot Teachavorasinskun
Associate Professor, Department of Civil Engineering, Faculty of Engineering,
Chulalongkorn University, Phayathai Rd., Pathumwan, Bangkok 10330, THAILAND.
Fax: 66-2-251-7304
e-mail : tsupot@chula.ac.th

and

Pulpong Pongvithayapanu
Graduate student, Department of Civil Engineering, Faculty of Engineering,
Chulalongkorn University, Bangkok, Thailand.
e-mail : srcpppn@ku.ac.th

Key words: Localization, shear wave velocity, sandy soil

INTRODUCTION

Localization is one of the most interesting phenomena for researchers studying of soil behaviors. Its uncertainty causes large variations in both stability and deformation of soils. In general, localization may be defined as the formation of a narrow shear band with intense straining; i.e. shear band. When shear band occurs, zone of discontinuity within soil mass is induced, which its physical properties are much more different from the others. A number of researches have been conducted to observe localization by sophisticated experiments, theoretical and numerical methods. Complicated instrumentations; e.g. Gamma-rays, Stereo-photogrammetry, X-ray Computed Tomography, Digital Image Analysis (DIA) and Digital Image Correlation (DIC), have been long applied to explore the characteristics within the localization zone (Roscoe, 1970; Desrues *et al.* 1996; Alshibli & sture, 1999; Sachan and Penumadu, 2007; Rechenmacher and Finno, 2004). Based on those, strain localization is recognized to be dependent on the initial states of effective stresses, void ratios, grain characteristics and stress history (Desrues & Viggiani, 2004).

Numerous studies on shear wave velocity of soils similar revealed that the initial states of effective stresses, void ratio, grain characteristics and stress history assert the most dominant influence on the shear wave velocity of soils (Roesler, 1979, Stokoe *et al.* 1995, Bellotti *et al.* 1996, Teachavorasinskun *et al.* 2002, Iwasaki *et al.* 1978, Hardin and Drenvich, 1972, Yu and Richart, 1984 and Teachavorasinskun and Akkarakun, 2004, Richart *et al.* 1970 and Santamarina *et al.* 2001). We may infer from these statements that strain localization and velocity of shear wave propagation are primarily dependent on some common key factors. It is therefore the main objective of this study to preliminary explore the evolution of localization in sandy soil by using shear wave propagation logging.

MATERIALS AND METHODS

The tested sand was taken from the eastern region of Thailand. Its grain particles were round to sub-angular shapes. The original sand was sieved to provide two batches of more uniform materials. The first batch (called herein *D16* sand) was that with grain size being greater than 1.18 mm (sieve No. 16). The other (*D40* sand) was sand that

passing through sieve No. 16 but retaining on sieve No. 40 (sieve opening = 0.425 mm). The physical properties and particle shapes of those two sands were summarized in Table 1 and Fig.1. Furthermore, commercially available silica sand conformed to the ASTM C-778 #20 – 30 was also tested in this study.

Air-dried sample was prepared by air-pluviation method from a specific height into the split mould having inner diameter and height of 5 and 10 cm. The initial suction of 10 *kPa* was then applied prior to removal of the mould. Consolidation was commenced on the air-dried sample by further applying of suction step-by-step to the prescribed confining pressure of 25, 50 and 80 *kPa*. Drained triaxial compression was then followed in the displacement controlled manner until sample encountering failure. Changes in radius of tested sample were manually measured at the marked locations on the sample.

During consolidation and shearing, velocities of shear wave and high resolution digital images were taken. Shear wave velocity was measured by a pair of bender elements installed at the top cap and pedestal at which their protrusion being 9.65 mm (Fig.2). Pulse excitation was given to the top bender element to generate shear wave. The transmitted pulse was received by the bottom bender element to indicate its arrival time as typically shown in Fig.3 (Lee and Santamarina, 2005 and Teachavorasinskun and Amornwithayalax, 2002).

A grid of 5×5 mm was attached on the surface of rubber membrane (Fig. 2a) in order to be used as references for digital image analysis (DIA). A series of high resolution images of 2848×2136 pixels were acquired correspondingly to the sequence of data acquisition. A simple digital image analysis (pixel analysis) was done in attempting to analyze local deformation of the grids around the observed localized areas.

RESULTS AND ANALYSIS

Shear wave velocity, V_s, is governed by the states of effective stresses which could be the mean effective stress (Teachavorasinskun and Amornwithayalax, 2002 and Teachavorasinskun *et al.* 2002) or those in the polarization plane (Roesler, 1979 and Yu and Richart, 1984). Fig. 4 depicts the variation of shear wave velocity against mean

effective stress during isotropic consolidation of tested samples. Since there was no existence of anisotropic stress, simple correlation between shear wave velocity, V_s, and mean effective stress (confining stress), $p' = (\sigma_1' + 2\sigma_3')/3$, can be attained as written in Eqn. (1).

$$V_s = \Theta\left(\frac{\sigma_1' + 2\sigma_3'}{3}\right)^{\zeta} \tag{1}$$

where Θ and ζ are constants and vary in the ranges of 85 – 100 and 0.16 – 0.23, respectively.

Relationships between the deviator stress, $q' = \sigma_1' - \sigma_3'$, and axial strain, ε_1, during drained compression were summarized in Fig. 5. The friction angles, $\phi = \arcsin[(\sigma_1' - \sigma_3')/(\sigma_1' + \sigma_3')]_{peak}$, varied in range of 42 - 44° for dense specimens and 39 - 40° for loose specimens of *D16* and *D40* sands. While slightly smaller friction angles of 35 - 39° was obtained for *silica* sand. For most samples, the peak deviator stress, by visual observation, occurred at the axial strain of about 3 to 5%.

Fig. 6 and 7 show the relations between shear wave velocity, V_s, and mean effective stress, $(\sigma_1' + 2\sigma_3')/3$, and deviator stress, $q' = \sigma_1' - \sigma_3'$, respectively. Both figures indicate that nor could effective mean stress or deviator stress express the pattern of shear wave velocity during drained shearing of sand. From those views, shear wave velocity of samples during shearing slightly increases during shearing. Notably that at very high levels of deviator stress, shear wave velocity shows very clear tendency of drastic reduction. This implies that drastic changes; i.e. localization, inside the sample.

Typical relationships between the stress ratio (q'/p') and V_s against the axial strain are shown in Fig. 8. V_s obtained from the very beginning part of shearing state increases according to axial strain (due to increasing of effective stresses). After axial strain reaches certain levels, i.e. $\varepsilon_a \approx 1 - 2\%$, V_s starts to decrease. This point is marked as *MVS* in the figure. The shear wave velocity reduces almost linearly with respect to increase in axial strain. It should be mentioned herein that the strain levels to mobilize

maximum stress ratio, $(q'/p')_{max}$ (marked by *MSR*), are greater than that required to attain *MVS*. This tendency implies that non-uniformity (initiation of strain localization) inside the specimen may occur before sample reaching its peak stress ratio. A similar trend was also observed from the experiment results of Anongphouth (2006). He performed a series of triaxial tests to explore the effect of stress-induced anisotropy on elastic shear modulus of Ping river sands by using bender elements. An example reproduced from his study was shown in Fig. 8(d). Based in his results, the axial strains require to attain *MVS* ranges between 0.93 – 1.90% and *MSR* occurs at around 3 – 6% which are comparable to those observed from other sands reported (see Table 2).

There are a number of conclusions stating the onset and formation of shear band. Desrues & Viggiani (2004) inferred from their plane strain compression tests on sand that the onset of a persistent shear band will always occur near, i.e. at or slightly before, the peak of stress ratio and never occurs after that peak. Finno *et al.* (1997) performed a series of plane strain compression on loose masonry sand and reported that no localization of strain was observed in the test before 2% of global axial strain. A wide zone of slight strain localization appears in the middle portion of the specimen when photographs at 2 – 3% of global axial strain are viewed in stereo.

Observation of digital images of local strain profiles taken during compression test can help identifying the onset and persistent of strain localization. Fig. 9 shows the relationship between stress ratio and shear wave velocity profile plotted against global axial strain (ε_a) and the corresponding images exhibiting the local strain profiles. From Fig. 9(b), at global axial strain of about 1.7%, local strains at some points inside the sample started to be greater than 5%. Note that *MVS* was reached at global strain of 1.3% (Fig. 9(a)). The observation infers that when strains of some parts of specimen exceeded 5%, intrinsic changes; i.e. localization, begin to dominate the behavior of sand. Furthermore, *MSR* would not be mobilized until some local area had been strained exceeding 10%. The conclusion that local strain of 5% and 10% are required to induce *MVS* and *MSR* could be drawn from other cases (Fig. 10 to 12). The only difference were that the global strains required to cause *MVS* and *MSR* were varied from case to case.

CONCLUSIONS

The investigation of strain localization of sandy soil samples by using shear wave propagation technique and the Digital Image Analysis (DIA) were performed in the triaxial compression test. Local sands and Silica sand of various grain sizes and shapes were employed in the study. The main results of the study are as follows;

1. The shear wave velocity increases as the isotropic confining pressure increases both in loose and dense conditions. Dense samples give slightly higher shear wave velocity than the loose ones at the same confining pressure.
2. Under shearing stage, shear wave velocity slightly increases at the very beginning part of the test. However, at high levels of stress ratio, the shear wave velocity tends to decline from its maximum value. It implies that the onset of strain localization starts from this point.
3. Shear wave velocity reduces almost linearly with the global axial strain. Local strain of exceeding 5% is required in order to attain the peak shear wave velocity. While local strain of 10% would be needed to mobilize peak stress ratio. It is therefore concluded that localization starts to dominate the behavior of soil when strain in some parts of sample become exceeding 5%. Detail exploration of shear wave velocity pattern is helpful in identification of initialization of shear band.

ACKNOWLEDGEMENTS

The authors would like to gratefully acknowledge the financial support provided by the Thailand Research Fund (TRF : RMU5180052) and by the Commission on Higher Education, Ministry of Education under Faculty Development Scholarship Program with the collaboration of AUN/SEED-Net.

REFERENCES

Alshibli, K.A. and Sture S. 1999. Sand shear band thickness measurement by Digital Image Techniques. Journal of Computing in Civil Engineering. 13(2): 103-109. ASCE.

Anongphouth, A. 2006. Effect of stress-induced anisotropy on elastic shear modulus of sands using bender elements. Master Thesis. Faculty of Engineering. Chulalongkorn University. Thailand.

Bellotti, R., Jamiolkowski, M., Lo Presti, D. C. F., and O'Neill, D.A. 1996. Anisotropy of small strain stiffness in Ticino sand. Géotechnique. 46(1): 115-131.

Desrues, J., Chambon, R., Mokni, M., and Mazerolle F. 1996. Void ratio evolution inside shear bands in triaxial sand specimens studied by computed tomography. Géotechnique. 46(3): 529-546.

Desrues, J. and Viggiani G. 2004. Strain localization in sand: an overview of the experimental results obtained in Grenoble using stereophotogrammetry. International Journal for Numerical and Analytical Methods in Geomechanics. 28(4): 279-321.

Finno, R., Harris, W., Mooney, M., and Vagina G. 1997. Shear bands in plane strain compression of loose sand. Géotechnique 47(1): 149-165.

Hardin, B.O. and Drnevich, V.P. 1972. Shear modulus and damping in soils: measurements and parameter effects. Journal of Soil Mechanics and Foundations Division. Terzaghi Lecture, 98(6): 603-624.

Iwasaki, T., Tatsuoka, F., and Takagi, Y. 1978. Shear moduli of sands under cyclic torsional shear loading. Soils and Foundations. 18(1): 39-56.

Lee J.S. and Santamarina J.C. 2005. Bender Elements: Performance and Signal Interpretation. Journal of Geotechnical and Geoenvironmental Engineering. 131(9): 1063-1070.

Rechenmacher, A.L. and Finno, R.J. 2004. Digital image correlation to evaluate shear banding in dilative sands. Geotechnical Testing Journal. 27(1): 13-22.

Richart, F.E., Hall, J.R., and Woods, R.D. 1970. Vibrations of Soils and Foundations. Prentice-Hall, Englewood Cliffs, N.J.

Roesler, S.K. 1979. Anisotropic shear modulus due to stress anisotropy. Journal of Soil Mechanics and Foundations Division. 105(7): 871-880.

Roscoe, K.H., 1970. The influence of strains in soil mechanics. Géotechnique. 20(2): 129-170.

Sachan, A. and Penumadu, D. 2007. Strain localization in solid cylindrical clay specimens using Digital Image Analysis (DIA) technique. Soils and Foundations. 47(1): 67-78.

Santamarina J.C., Klein K.A., and Fam, M.A. 2001. Soils and Waves: Particulate Materials Behavior, Characterization and Process Monitoring. J. Wiley & Sons, 508 pages.

Stokoe, K.H. II, Hwang, S.K., Lee, J.N.K., and Andrus, R.D. 1995. Effects of various parameters on the stiffness and damping of soils at small to medium strains. in Shibuya et al. (Eds). Proceedings of the International Symposium on Pre-failure Deformation of Geomaterials. Vol. 2: 785–816.

Teachavorasinskun, S. and Akkarakun, T. 2004. Paths of elastic shear modulus of clays" Géotechnique. 54(5): 331-333.

Teachavorasinskun, S., Thongchim, P., and Lukkunaprasit P. 2002. Shear modulus and damping of soft Bangkok clays. Canadian Geotechnical Journal. 39: 1201–1208.

Teachavorasinskun, S. and Amornwithayalax, T. 2002. Elastic shear modulus of Bangkok clay during undrained triaxial compression. Géotechnique. 52(7): 537-540.

Yu, P. and Richart, F.E. 1984. Stress ratio effects on shear modulus of dry sands. ASCE Journal of Geotechnical Engineering. 110(3): 331–345.

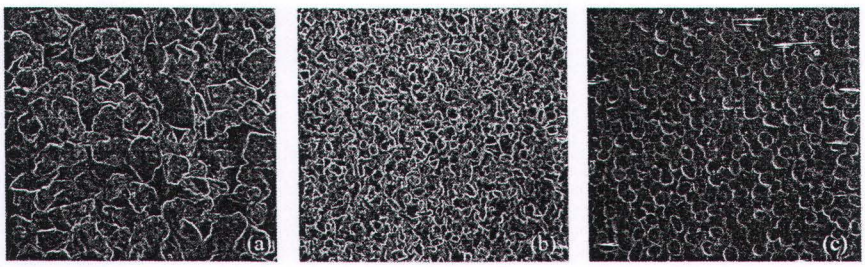

Fig. 1 Shapes of grain particles of (a) *D16*, (b) *D40* and (c) *Silica* sands.

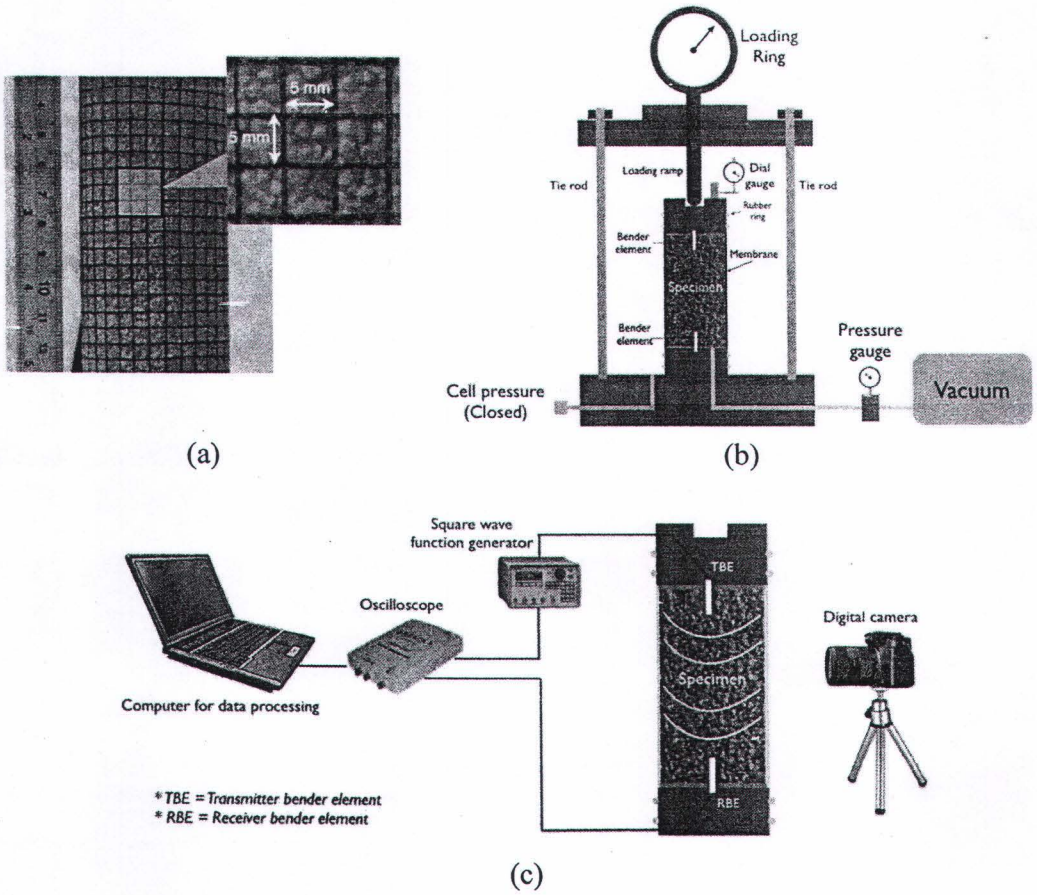

Fig.2 General arrangement of equipment used in the study (a) the square grid of 5×5 mm mounted on the outer surface of rubber membrane, (b) schematic view of triaxial equipment used in the study and (c) schematic view of the bender element setup.

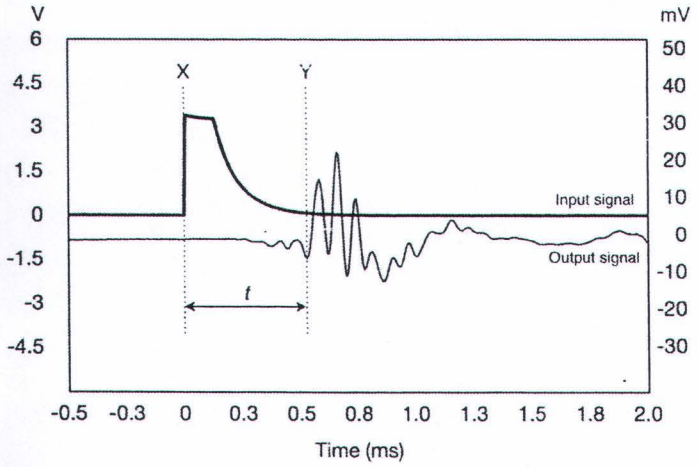

Fig.3 Typical interpretation propagation of shear wave in tested sample.

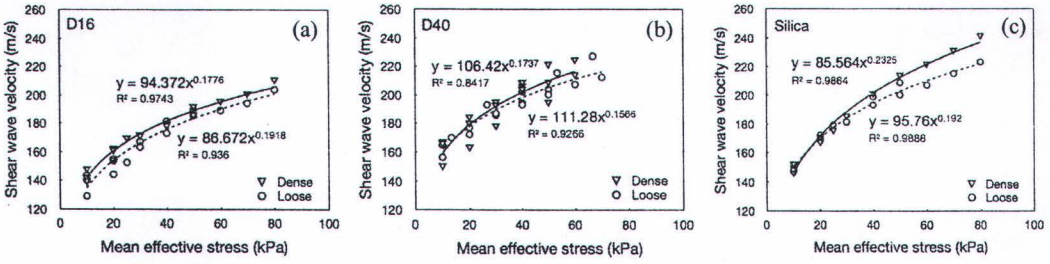

Fig. 4 Shear wave velocity and stress relation in loose and dense conditions and its empirical relation for (a) *D16* (b) *D40* and (c) *Silica* sand

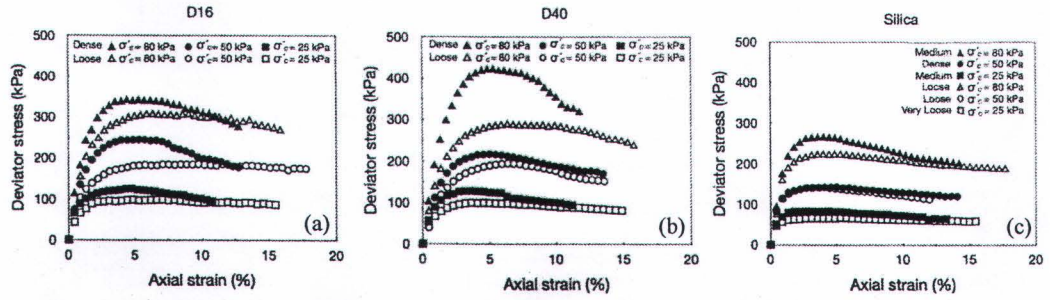

Fig. 5 Stress strain responses from triaxial tests in various initial state conditions obtained from (a) *D16* (b) *D40* and (c) *Silica* sand

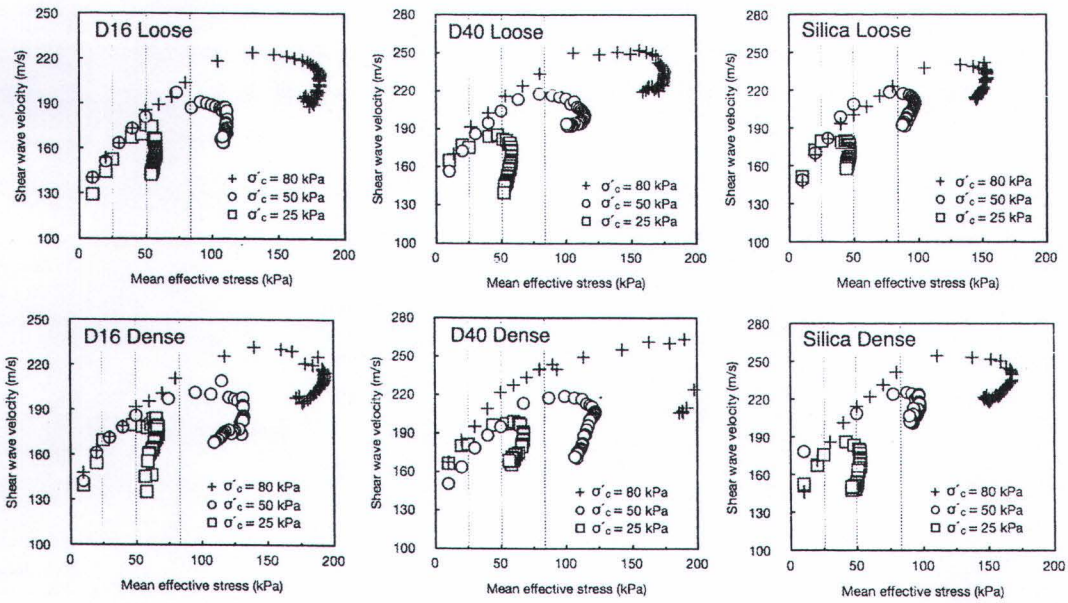

Fig. 6 Influence of mean effective stress to shear wave velocity on *D16*, *D40* and *Silica* sand in various confining conditions

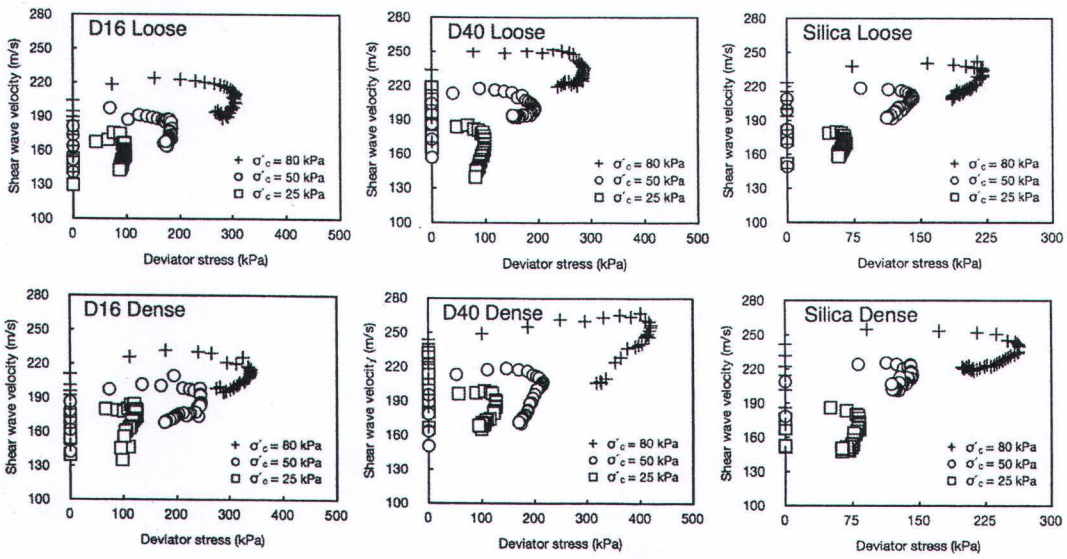

Fig. 7 Influence of deviator stress to shear wave velocity on *D16*, *D40* and *Silica* sand in various confining conditions

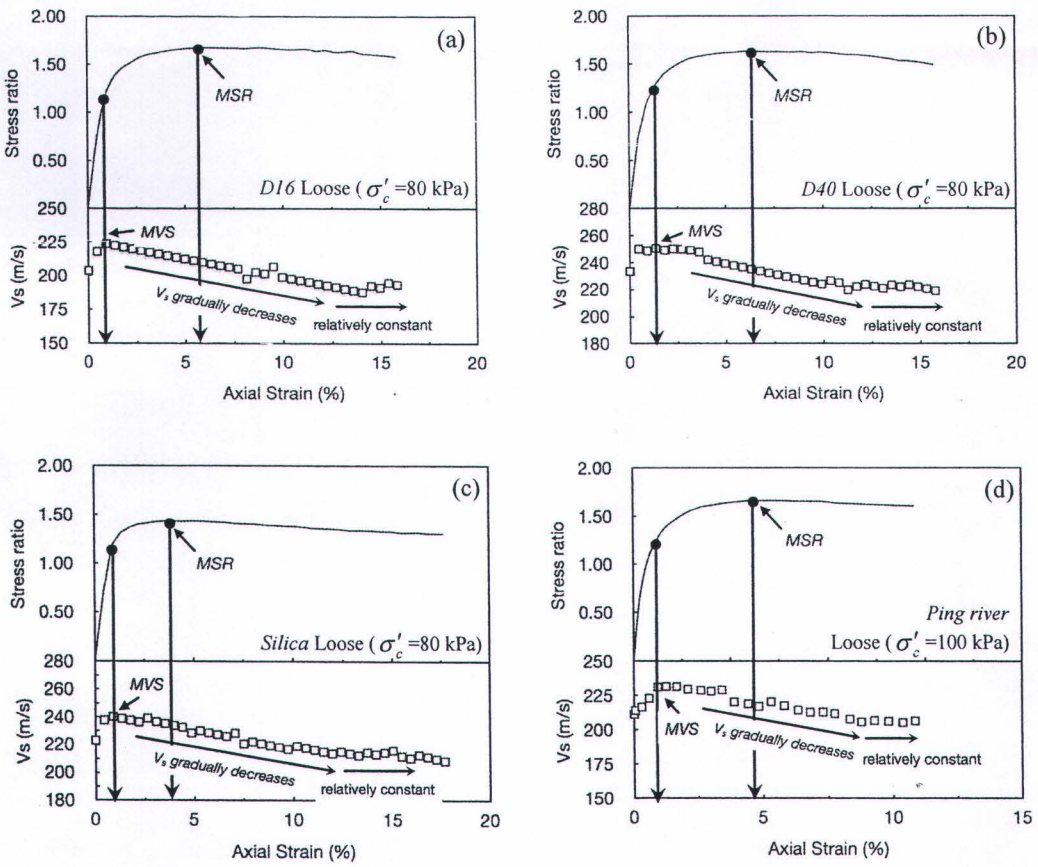

Fig. 8 Relationship between stress ratio and V_s versus axial strain during compression test inside loose sand samples of (a) *D16* (σ'_c= 80 kPa), (b) *D40* (σ'_c= 80 kPa), (c) *Silica* (σ'_c= 80 kPa) and (d) *Ping river* (σ'_c= 100 kPa) samples

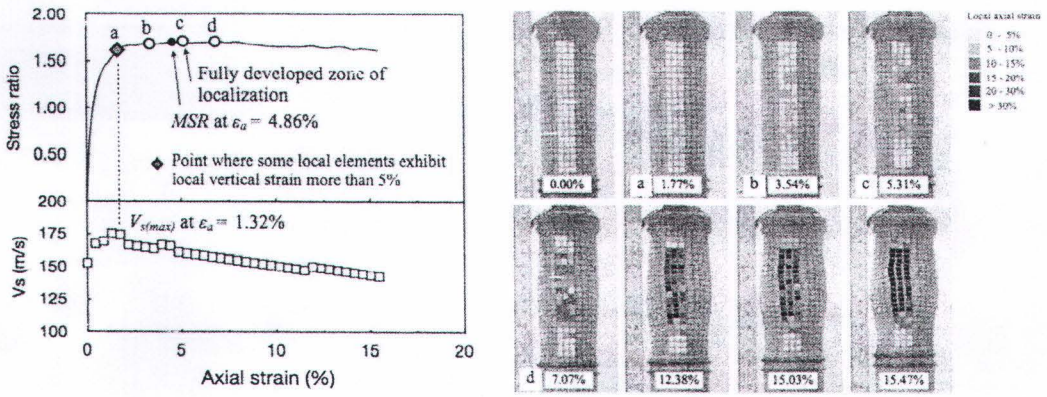

Fig. 9 (a) Stress ratio and shear wave velocity profile plotted against global axial strain (b) Local strain profile of *D16* sample in loose state (σ'_c = 25 kPa)

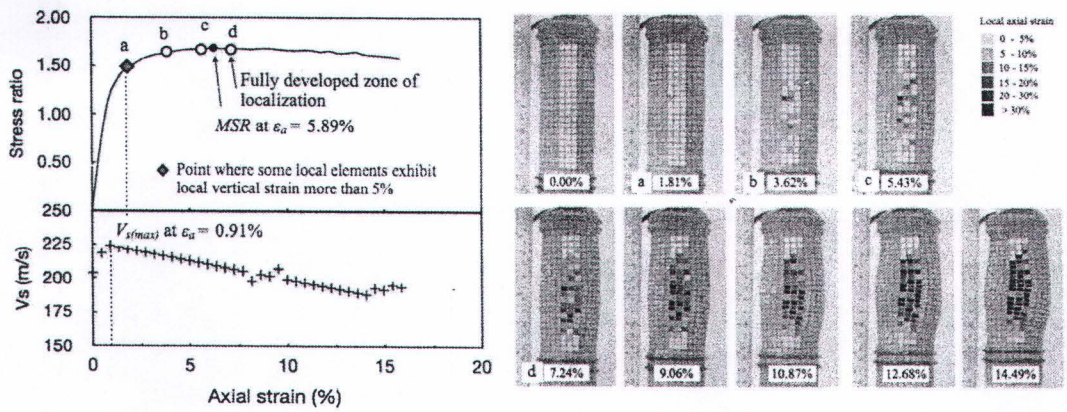

Fig. 10 (a) Stress ratio and shear wave velocity profile plotted against global axial strain (b) Local strain profile of *D16* sample in loose state (σ'_c = 80 kPa)

Table 1 Basic physical properties of tested sands

Basic property	***D16***	***D40***	***Silica***
Shape of grain particle	Low to medium sphericity with angular shape	Low to medium sphericity with angular shape	High sphericity with well rounded shape
Mean size particle, d_{50} (mm)	1.18	0.465	0.60
Specific gravity, G_s	2.69	2.72	2.65
Maximum void ratio, e_{max}	1.06	1.12	0.6
Minimum void ratio, e_{min}	0.713	0.808	0.459

Table 2 Summary of levels of axial strains to attain *MVS* and *MSR*

Sand	**Density**	**Axial strain to *MVS* (%)**			**Axial strain to *MSR* (%)**			**Slope after *MVS* (m_v)**		
Confining pressure		25 kPa	50 kPa	80 kPa	25 kPa	50 kPa	80 kPa	25 kPa	50 kPa	80 kPa
D16	Loose	1.32	0.45	0.91	4.86	5.89	5.89	-2.52	-2.02	-2.75
	Dense	2.15	0.65	0.88	4.75	5.22	4.40	-3.73	-3.62	-3.77
D40	Loose	0.90	1.36	1.42	3.61	6.34	6.31	-3.15	-2.84	-3.56
	Dense	1.34	1.33	1.12	3.58	4.88	5.22	-4.49	-4.03	-4.58
Silica	Loose	0.88	0.44	0.88	3.09	3.99	3.98	-1.61	-2.18	-2.03
	Dense	0.44	0.91	0.44	4.41	4.99	4.00	-2.26	-2.38	-2.58
Confining pressure		100 kPa	200 kPa	300 kPa	100 kPa	200 kPa	300 kPa	100 kPa	200 kPa	300 kPa
****Ping river***	Loose	1.07	1.10	1.55	4.66	6.12	6.31	-3.17	-2.43	-2.33
	Dense	0.93	1.90	1.45	3.18	3.78	4.21	-3.60	-3.13	-4.10

* Ping river sand taken from the northern part of Thailand, d_{50} = 0.44 mm, G_s = 2.65, e_{max} = 0.86 and e_{min} = 0.53 (Anongphouth, 2006)